AEROELASTIC CONTROL OF HELICOPTER BLADE SAILING USING SHAPE MEMORY ALLOY

Vinícius Piccirillo, Luiz Carlos Sandoval Goes and Roberto Luiz da Cunha Barroso Ramos
Technological Institute of Aeronautics, 12228-900 São José dos Campos, SP, Brazil

***Abstract* — This paper analyzes the unsteady flow response of a helicopter blade-sailing control system using shape memory alloy (SMA). The aeroelastic analysis focuses on the performance of a proposed semi-active controller with respect to the reduction of blade flapping vibrations in articulated rotors during engagement shipboard operations. The designed control yields gust load alleviation by increasing the stiffness of the flapping motion. The simulation results show that the proposed SMA aeroelastic controller can yield tunnel-strike suppression and significant reduction in upward blade tip deflections at the unsteady wind-over-deck conditions of interest.**

***Keywords* — Helicopter blade sailing, aeroelasticity, shape memory alloy, unsteady flow.**

I. INTRODUÇÃO

Flow-induced unsteady loads are often related to large vibrations and damage in flexible structures. Shipboard helicopters, operating in the hostile maritime environment from frigate-like platforms, are especially susceptible to these effects during rotor engagement/disengagement operations under high wind-over-deck (WOD) conditions. These dangerous conditions are amplified by the ship structure, which generates flow velocity gradients and vortices over the flight deck. Therefore, shipboard helicopter operations are among the most hazardous military operations and the shipboard environment imposes severe restrictions on the missions and determines stringent requirements for the design of aerial vehicles.

The problem of flight in the vicinity of ships is usually called Dynamic Interface (DI) problem [1]. Among the dynamic phenomena in the DI that must be analyzed and controlled, one is especially important for rotary-wing aircraft: *blade sailing*.

Blade sailing is an aeroelastic transient phenomenon characterized by the occurrence of large flapping vibrations, possibly associated with tunnel/tail-boom strikes, due to fluid-structure interactions during engagement or disengagement operations of helicopter rotors under high wind conditions [2].

Vinícius Piccirillo, pcmec@ita.br, Luiz Carlos Sandoval Goes, goes@ita.br, Roberto Luiz da Cunha Barroso Ramos, rlcbramos@gmail.com

The blade-sailing control problem has a theoretical importance, due to the nonlinear time-varying characteristics of the associated blade flapping oscillator, which is also subjected to large disturbances.

Considering the ubiquitous use of the shipboard helicopter in critical defense missions, the problem has a practical relevance as well, as shown by a recent NATO symposium about the study of flow-induced unsteady loads and the impact on military applications [3]. The obtained theoretical results may be helpful for better understanding of helicopter blade-sailing alleviation using a shape memory alloy (SMA) element considering several fluctuation flow conditions.

II. SMA CONSTITUTIVE MODEL

To describe the behavior of the shape memory alloy, the constitutive model proposed by [4] is adopted. This model is based on Devonshire theory and it defines a free energy of Helmholtz (ψ) in the polynomial form and it is capable to describe the shape memory and pseudoelasticity effects. The polynomial model is suitable for one-dimensional cases and it does not consider an explicit potential of dissipation, and no internal variable is considered. On this form, the free energy depends only on the observable state variables (temperature (T) and strain (ε)), that is, $\psi = \psi(\varepsilon, T)$.

The free energy is defined in such way that, for high temperatures ($T > T_A$), the energy has only one point of minimum corresponding to the null strain representing the stability of the austenite phase (A); for intermediate temperatures ($T_M < T < T_A$) it presents three points of minimum corresponding to the austenitic phase (A), and two martensitic phases (M^+ and M^-), which are induced by positive and negative stress fields, respectively; for low temperature ($T < T_M$), there are two points of minimum representing the two variants of martensite (M^+ and M^-), corresponding to the null strain.

Therefore, the above restrictions are given by the following polynomial equation:

$$\rho\psi(\varepsilon, T) = \frac{1}{2}q(T - T_M)\varepsilon^2 - \frac{1}{4}b\varepsilon^4 + \frac{1}{6}e\varepsilon^6 \qquad (1)$$

where q and b are constants of the material, T_M corresponds to the temperature where the martensitic phase is stable, ρ is the SMA density, and the free energy has only one minimum at zero strain. The constant e may be expressed in terms of other constants of the material:

$$T_A = T_M + \frac{b^2}{4qe}, \quad (2)$$

where T_A corresponds to the temperature where the austenite phase is stable. Thus, the stress-strains relation is given by:

$$\sigma = q(T - T_M)\varepsilon - b\varepsilon^3 + \frac{b^2}{4q(T_A - T_M)}\varepsilon^5 \quad (3)$$

According to [5], the polynomial model represents, in a qualitatively coherent way, both martensite detwinning process and pseudoelasticity, although it does not consider twinned martensite (M). In other words, there is no stable phase for $T < T_M$ in a stress-free state, but the authors believe that this analysis is useful to the understanding of the nonlinear dynamics of shape memory systems. The proposed model captures itself all of the essential features of the pseudoelasticity phenomenon for blade-sailing control.

III. AEROELASTIC MODELING

For control purposes the blade-sailing aeroelastic model can be greatly simplified by considering the forces and moments actuating only in the flapping plane.

Fig. 1 shows the forces at a blade element for the simplified blade-sailing planar model, according to a frame rotating with the blade. The simplified diagram of forces at a planar blade element [6] in Fig. 1 illustrates the main factors that govern the blade-sailing behavior.

Ship motion effects are not included. The resulting moments about the flapping hinge in conjunction with the droop/flap stop effects, modeled as a nonlinear rotational spring, determine the blade tip deflections related to the angle *β*.

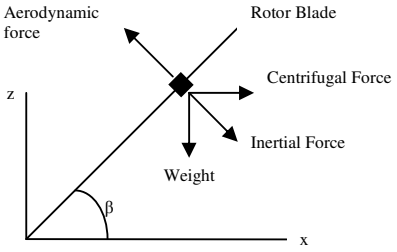

Figure 1: Forces at a flapping planar blade element for the proposed blade-sailing model (rotating frame)

Fig. 2 shows the flow velocity components in the plane of the rotor for the proposed blade-sailing model, considering the WOD conditions. V_{WOD} and Ψ_{WOD} are, respectively, the magnitude and direction of the incoming wind velocity with respect to the ship centerline

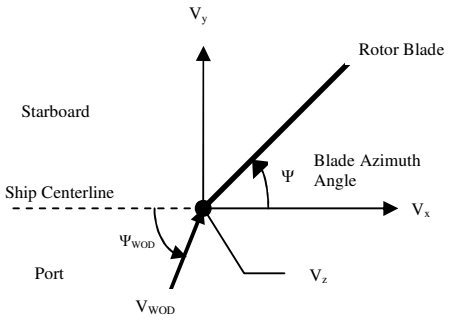

Figure 2: Flow velocity components for the WOD conditions

The blade-sailing modeling is based on a proposed rotary-wing aeroelastic scheme applied to articulated shipboard rotor blades, according to the Figs. 1 and 2, taking into account some simplifying assumptions [7]-[9].

Generally, the flow field that affects the rotor behavior is non-uniform and unsteady, thus, the three velocity components vary with space and time. Mean flow velocity gradients arise due to the ship geometry and the fluctuating flow velocity components arise due to the ship geometry and also to the meteorological effects, like turbulence from storms.

To simplify the aeroelastic analysis, only the lateral (90^o or 270^o) wind condition is considered, focusing the ship airwake modeling on the effects of the horizontal and vertical velocity components related to this worst-case blade-sailing condition [2]. The WOD velocity component V_x is neglected. For a typical frigate-like configuration with only one flight deck, as considered in this work, the WOD horizontal velocity V_y for the lateral condition can be considered uniform along the shipboard rotor.

The mean flow vertical velocity related to the interaction between the lateral undisturbed wind flow and a typical frigate-like structure can be approximated by a linear distribution along the flight deck and the helicopter rotor [10]-[11]. Therefore, for a rotor blade element at radial station r and azimuth Ψ, and constant WOD horizontal velocity component V_y, the WOD mean vertical velocity, according to the linear distribution approximation ("linear gust model"), is given by:

$$\overline{V_z} = K_v V_y \frac{r}{R} \sin\Psi . \quad (4)$$

Unsteady flow effects can be modeled by considering a sinusoidal gust across the rotor disk for the WOD fluctuating vertical velocity component, representing the effects of the dominant frequency ω_f of the ship airwake on the helicopter rotor, as follows:

$$V_z' = K_f V_y \sin\omega_f t . \quad (5)$$

The gust amplitude parameters K_v and K_f, and the sinusoidal gust frequency ω_f govern the flow-induced unsteady loads associated with the WOD vertical velocity component, which characterizes a flow field over the flight deck that varies with space and time according to Eqs. 4 and 5. The aerodynamic components affecting a shipboard rotor

blade can be calculated according to the blade-element theory, as follows [12]:

$$V_x = V_{WOD}\cos\Psi_{WOD}, \quad V_y = V_{WOD}\sin\Psi_{WOD},$$
$$U_T = \Omega r - V_y\cos\Psi + V_x\sin\Psi, \qquad (6)$$
$$U_P = r\dot{\beta} + (V_y\sin\Psi + V_x\cos\Psi)\beta - V_z$$

In particular, Ψ_{WOD} is equal to 90° for lateral port side winds and to 270° for lateral starboard side winds. U_P and U_T are, respectively, the normal and tangential flow velocity components at the blade element at radial station r, azimuth Ψ and flapping angle β.

Smart materials can be applied to the reduction of blade-sailing vibrations by means of flapping stiffness effect. As mentioned in the introduction, previous researches on blade-sailing active control were based on swashplate actuation [12], trailing edge flaps [13], active twist [14] and individual blade root control [7]-[9].

Introducing the shape memory alloy stiffness effect:

$$\ddot{\beta} + \frac{\gamma\Omega}{8}\left[1+\frac{4}{3}\left(\mu_x\sin\Psi-\mu_y\cos\Psi\right)\right]\dot{\beta} + \Omega^2\left\{1+\frac{\gamma}{8}\left[\frac{4}{3}\left(\mu_x\cos\Psi+\mu_y\sin\Psi\right)-\right.\right.$$
$$\left.\left.-\left(\mu_y^2-\mu_x^2\right)\sin 2\Psi - 2\mu_x\mu_y\cos 2\Psi\right]\right\}\beta + \sigma_1(\beta) + K_{SMA}(\beta,T) =$$
$$\frac{\gamma\Omega^2}{8}\left[1+\frac{8}{3}\left(\mu_x\sin\Psi-\mu_y\cos\Psi\right)+2\left(\mu_x\sin\Psi-\mu_y\cos\Psi\right)^2\right]\theta_u$$
$$+\frac{\gamma\Omega^2}{8}\left[1+\frac{8}{3}\left(\mu_x\sin\Psi-\mu_y\cos\Psi\right)+2\left(\mu_x\sin\Psi-\mu_y\cos\Psi\right)^2\right]\theta_i +$$
$$\frac{\gamma\Omega^2}{2}\left[\frac{1}{5}+\frac{1}{2}\left(\mu_x\sin\Psi-\mu_y\cos\Psi\right)+\frac{1}{3}\left(\mu_x\sin\Psi-\mu_y\cos\Psi\right)^2\right]\theta_{tw}$$
$$+\frac{\gamma\Omega}{8R}\left\{\left[1+\frac{4}{3}\left(\mu_x\sin\Psi-\mu_y\cos\Psi\right)\right]V_{zg}+\left[\frac{4}{3}+2\left(\mu_x\sin\Psi-\mu_y\cos\Psi\right)\right]V_{zu}\right\}-\frac{3}{2R}g \qquad (7)$$

Note, in Eq. (7), that the restitution force may be expressed as $K_{SMA} = \sigma A$, where A is the area of the SMA element, which is placed at the blade root.

IV. MODEL VERIFICATION AND NUMERICAL SIMULATION

The verification of the blade-sailing model given by Eq. 7 is obtained by comparison with results given in [12] and [10] from models validated with experimental data, according to a fourth-fifth order Runge-Kutta numerical simulation. Table 1 show the parameter values for the simulations, which are based on the H-46 Sea Knight shipboard helicopter characteristics, in conjunction with a WOD linear gust parameter K_y equal to 0.25.

Table 1: Parameters for the model verification

γ (Lock number)	7.96
Ω_0 (nominal rotor rotational speed)	27.65 rad/s
V_y (lateral WOD velocity)	- 42.5 kt
V_x (longitudinal WOD velocity)	0 kt
R (rotor radius)	25.5 ft
ω_{nr} (blade non-rotating flapping frequency)	6 rad/s
β_{DS} (droop stop angle)	- 1°
B_{FS} (flap stop angle)	1°
$\theta_{.75}$ (collective pitch angle)	3°
θ_{tw} (built-in twist angle)	- 8.5°
θ_{1s} (longitudinal cyclic angle)	2.5°
θ_{1c} (lateral cyclic angle)	0.0693°

A numerical simulation is carried out for the linear gust model of the ship airwake and Fig. 3 illustrates the results.

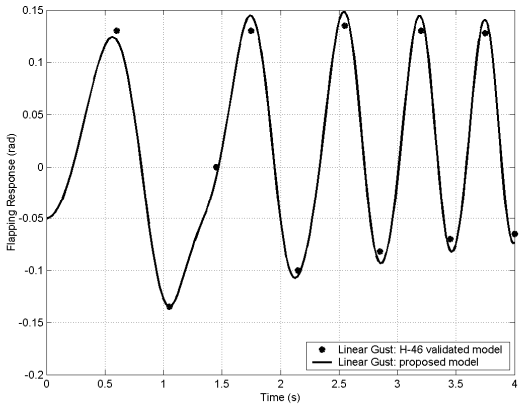

Figure 3: Flapping response for the linear gust model

The flapping response diagram in Fig. 1 shows a very good agreement of the proposed model with the results given in [10]. The time range 0-4 seconds of the simulation corresponds to 6-10 seconds for the actual H-46 engagement behavior, when rotor rotational speeds are low, varying from 10% to 46% of the nominal rotation speed (NR).

As the shape memory alloy presents different properties, depending on the temperature, a study on the pseudoelastic dynamic behavior is presented, considering a higher temperature, where austenitic phase is stable in the alloy. In all simulations, in order to analyze the behavior of the aeroelastic dynamical system, the spring is assumed to be made of a Ni-Ti alloy and the properties are presented in Table 2 [5]. In this case, it is used a temperature of the alloy around $T = 315K$ (approximately $T \approx 42°C$), and is assumed a SMA element with $A = 10^{-5}\,m^2$.

Table 2. Material constants for a Ni-Ti alloy

Parameter	Units	Values
q	MPa/K	1000
b	Mpa	40×10^6
T_M	K	287
T_A	K	313

The performance of a blade-sailing controller using a SMA spring is then analyzed considering unsteady flow effects. Fig.4 shows the flapping response of the sinusoidal gust for an incoming wind velocity V_{WOD} of 50 kt (nominal value) and for the frequency of 5 rad/s. In this case, the significant blade sailing reduction is observed.

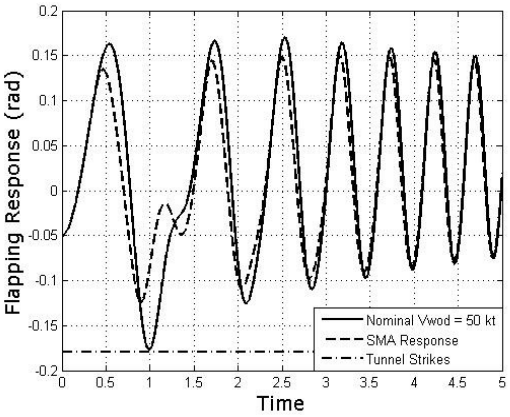

Figure 4: SMA response for K_f = 0.1 and ω_f =5 rad/s,

Now, the next simulations illustrates the case when occur the fluctuation flow condition in relation to nominal value of V_{WOD}. In figs. 5, 6, 7 and 8, the fluctuation flow corresponds to 5%, 10%, 15% and 20% respectively of the nominal value. Note that in all situation the system present a blade sailing phenomena but when is introduced a SMA element in the system and considering the temperature of alloy in approximately $42°C$ a significant reduction of flapping vibration is observed in all cases.

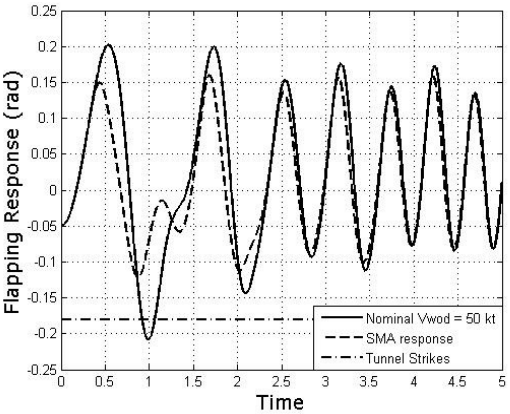

Figure 5: SMA response for K_f = 0.1, ω_f =5 rad/s, and fluctuation flow of 5%

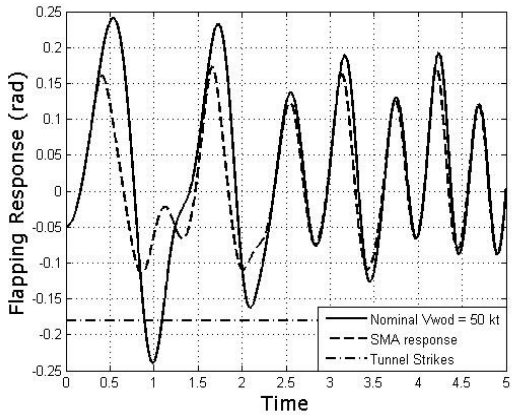

Figure 6: SMA response for K_f = 0.1, ω_f =5 rad/s, and fluctuation flow of 10%

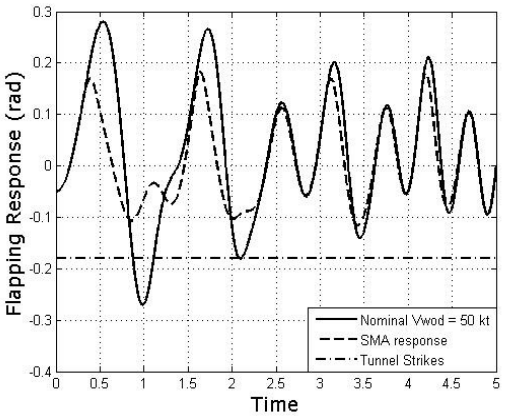

Figure 7: SMA response for K_f = 0.1, ω_f =5 rad/s, and fluctuation flow of 15%

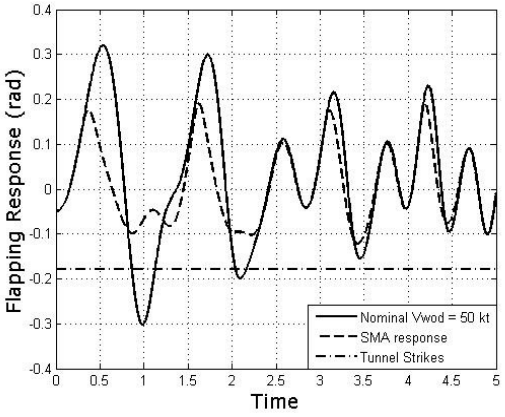

Figure 8: SMA response for K_f = 0.1, ω_f =5 rad/s and fluctuation flow of 20%

V. CONCLUSIONS

This paper analyzed the influence of SMA element controllers on the helicopter blade-sailing phenomenon. A study on the pseudoelastic behavior of a SMA element was presented, considering a higher temperature, where austenitic

phase is stable in the alloy. The simulations showed that a temperature-controlled SMA element can compensate high lift conditions during engagement shipboard operations by modifying the stiffness properties of the flapping oscillator.

The results showed that a SMA device can significantly reduce the blade-sailing vibrations, avoiding tunnel-strike occurrences at severe unsteady flow conditions and for several fluctuation flow conditions.

REFERENCES

[1]Rhoades, M.M., Healey, J.V., 1992, "Flight deck aerodynamics of a nonaviation ship". Journal of Aircraft, v. 29, n. 4, p. 619-626, Jul.-Aug.

[2]Newman, S.J., 1995, "The Verification of a Theoretical Helicopter Rotor Blade Sailing Method by Means of Windtunnel Testing". The Aeronautical Journal of the Royal Aeronautical Society, v. 99, n. 982, p. 41-51.

[3]Wall, A.S., Zan, S.J, Langlois, R.G., Afagh F.F., 2005, "A Numerical Model for Studying Helicopter Blade Sailing in an Unsteady Airwake". In: Flow-Induced Unsteady Loads and the Impact on Military Applications – NATO symposium.

[4]Savi, M., and Braga, A.M.B., 1993, "Chaotic Vibrations of an Oscillator with Shape Memory", Journal of the Brazilian Society of Mechanical Sciences and Engineering, Vol. XV, pp. 1 – 20.

[5]Paiva, A., Savi, M.A., 2006, "An Overview of Constitutive Models for Shape Memory Alloy", Mathematical Problem in Engineering, Vol. 2006, pp. 1 – 30.

[6]Johnson, W. Helicopter Theory. [S.l.]: Dover, 1994, p. 1-767.

[7]Ramos, R. L. C. B., 2007, "Aeroservoelastic Analysis of the Blade-Sailing Phenomenon in the Helicopter-Ship Dynamic Interface". Thesis (D.Sc.) – Technological Institute of Aeronautics, Brazil.

[8]Ramos, R.L.C.B., de Andrade, D., Goes, L.C.S., 2009a, "Individual Blade Root Control of Helicopter Blade Sailing for Articulated Shipboard Rotors", 65th American Helicopter Society Annual Forum.

[9]Ramos, R.L.C.B., de Andrade, D., Goes, L.C.S., 2009b, Aeroservoelastic Analysis of a Proposed Helicopter Blade- Sailing Feedback Control System in Unsteady Flow, 8th Brazilian Conference on Dynamics, Control and Applications, Bauru, May 18-22.

[10]Geyer JR., W.P., Smith, E.C., Keller, J.A., 1998, "Aeroelastic Analysis of Transient Blade Dynamics During Shipboard Engage/Disengage Operations". Journal of Aircraft, v. 35, n. 3, p. 445-453.

[11]Newman, S.J., 1990, "A Theoretical Model for Predicting the Blade Sailing Behaviour of a Semi-Rigid Rotor Helicopter". Vertica, 14, (4), p. 531-544.

[12] Keller, J.A., 2001, "Analysis and control of the transient aeroelastic response of rotors during shipboard engagement and disengagement operations". Thesis (PhD) - The Pennsylvania State University.

[13]Jones, M.P., Newman, S.J., 2007, "A Method of Reducing Blade Sailing through the Use of Trailing Edge Flaps". In: American Helicopter Society Annual Forum, 63.

[14]Khouli, F., Wall, A.S., Langlois, R.G., Afagh F.F., 2008, "Investigation of the Feasibility of a Proposed Hybrid Passive and Active Control Strategy for the Transient Aeroelastic Response of Helicopter Rotor Blades During Shipboard Engage and Disengage Operations". In: American Helicopter Society Annual Forum, 64.